

PROCEEDINGS

28TH RCI INTERNATIONAL CONVENTION AND TRADE SHOW

CONDENSATION RISK OF MECHANICALLY ATTACHED ROOF SYSTEMS IN COLD-CLIMATE ZONES

MANFRED KEHRER

OAK RIDGE NATIONAL LABORATORY

P.O. Box 2008, Oak Ridge, TN 37831

Phone: 865 576-3924 • Fax: 865-574-9354 • E-mail: kehrerm@ornl.gov

SIMON PALLIN, LICENG

CHALMERS UNIVERSITY OF TECHNOLOGY, SWEDEN

595 English Village Way, Knoxville, TN 37919

Phone: (865) 232-9168 • E-mail: simon.pallin@chalmers.se



ABSTRACT

Flat roofs generally have a high potential of nightly overcooling and, therefore, an increased risk of condensation within the construction, particularly in cold-climate zones, depending on their specific assembly. A white exterior surface or so-called “cool roof,” applied to decrease cooling loads and to save energy, increases the condensation risk due to lower energy gains during daylight hours. There have been questions raised about the sustainability of using cool membranes in northern U.S. climate zones due to the potential of moisture accumulation below the membrane. Transient hygrothermal simulation using real climate data is state-of-the art today and can help to study different effects. Results will be shown.

SPEAKERS

MANFRED KEHRER — OAK RIDGE NATIONAL LABORATORY - OAK RIDGE, TN

MANFRED KEHRER received his diploma in technical physics in 1993 from the University of Applied Science in Munich, Germany. After that, he worked at Fraunhofer IBP, Germany, for ten years in the laboratory of the department of hygrothermics, where he studied hygrothermal laboratory and field measurements. Eventually, he moved into the software development group of the department, where he started to work on modeling, programming, and testing of transient hygrothermal transport calculations (WUFI). In 2005, he became manager of that group and was responsible for the development, quality control, and sales of WUFI products and was heavily involved in many collaborative projects worldwide. Since 2011, he has worked as a senior researcher within the Building Envelopes Group at the Oak Ridge National Laboratory, TN, where he is in charge of hygrothermal investigations. He is a voting member of ASTM C16 and E06, a member of ASHRAE TC 4.4, and on the editorial board of the *Journal of Building Physics*. In 2011, Kehr, together with his development team at Fraunhofer IBP, was awarded the Moisture Safety Prize from the Moisture Research Center at Lund University, Sweden.

SIMON PALLIN, LICENG — CHALMERS UNIVERSITY OF TECHNOLOGY, SWEDEN - KNOXVILLE, TN

SIMON PALLIN was a medical student for 1½ years before studying to become a civil engineer, and he also owned a fitness center for six years, managing about 40 employees. As part of his master's degree work, he studied at California State University of Long Beach with a focus on reinforced masonry design and interior design. In 2009, after completing his master's thesis, Pallin was employed by Chalmers University of Sweden as a full-time PhD student, studying risks coupled to changes in air movements and moisture safety when performing retrofitting measures in residential buildings. He has performed simulations of residential moisture production rates and quantitative probabilistic risk analyses of heat, air, and moisture transfer in different residential retrofitting techniques, with an emphasis on energy consumption and moisture safety. In 2012, Simon was awarded with a scholarship by the Sweden-America Foundation for a six-month research opportunity at Oak Ridge National Laboratory.

CONDENSATION RISK OF MECHANICALLY ATTACHED ROOF SYSTEMS IN COLD-CLIMATE ZONES

BACKGROUND

A white or “cool” roof is constructed to decrease thermal loads from solar radiation, therefore saving energy by decreasing cooling demands. Unfortunately, cool roofs with a mechanically attached membrane have shown a higher risk of intermediate condensation in the materials below the membrane in certain climates (Ennis & Kehrer, 2011) and in comparison with similar constructions with a darker exterior surface (Bludau, Zirkelbach, & Kuenzel, 2009). As a consequence, questions have been raised regarding the sustainability and reliability of using cool roof membranes in northern U.S. climate zones.

A white roof surface reflects more of the incident solar radiation than a dark surface, making a distinguishable difference in the surface temperature of the roof. However, flat roofs facing a clear sky, with either a light or a dark surface, are constantly losing energy to the atmosphere due to the exchange of infrared radiation. This phenomenon exists during both the night and the day. During the day, if the sun shines on the roof surface, the exchange of infrared radiation typically becomes insignificant. During the night and in cold climates, the temperatures of the roof surface and the air can differ by as much as 68°F (20°C) (Hagentoft, 2001), which could result in a roof surface temperature that is much colder than the ambient temperature. Further, a colder roof surface has increased energy loss and risk of condensation in the building materials below the membrane. Therefore, both light- and dark-coated roof membranes are cooled by infrared radiation exchange during the night, though a darker membrane is heated more by solar radiation during the day, thus decreasing the risk of condensation.

The phenomenon of nighttime cooling and the lack of solar gain during the day are not likely the exclusive issues affecting the risk of condensation in cool roofs with mechanically attached membranes. Roof

systems with thermoplastic membranes are prone to be more affected by interior air intrusion into the roof structure, both from wind-induced pressure differences and from the flexibility and elasticity of the membrane (Molleti, Baskaran, Kalingar, & Beaulieu, 2011). Depending on the air permeability of the material underneath the membrane, wind forces increase the risk of fluttering (also referred to as billowing) of a flexible single-ply thermoplastic membrane. As expected, the wind-induced pressure differences create a convective air flow into the structure (i.e., air intrusion). If the conditions are right, moisture from the exchanging air may condense on surfaces with a temperature below the dew point.

The definite path of convective air flow through the building envelope is usually very difficult to determine, so simplified models (Künzel, Zirkelbach, & Schafaczek, 2011) help to estimate the additional moisture loads caused by air intrusion. The wind-uplifting pressure, in combination with wind gusts, are important factors for a fluttering roof. Unfortunately, the effect of fluctuating wind is difficult to estimate, as this is a dynamic phenomenon, and existing standards (ASTM, 2011a) take into account only a steady-state approach (i.e., there are no guidelines or regulations on how to estimate the air intrusion rate). Obviously,

more detailed knowledge on the hygrothermal performance of mechanically attached cool roof systems is needed with regard to surface colors, roof airtightness, climate zones, and indoor moisture supply.

INTRODUCTION

The hygrothermal performance of the aforementioned mechanically attached roof system has been investigated with numerical simulations. Measurements of the airtightness of the roof construction are necessary (see “Air Intrusion” in the section on “Air Intrusion”) to provide reliable input data for simulations. Studying these phenomena requires a tool capable of modeling heat and moisture transport in a transient simulation and with realistic boundary conditions. Long-wave (infrared) radiation must be considered at the exterior surface; otherwise, nightly overcooling cannot be taken into account in the simulations of a cool roof. On account of these prerequisites, the hygrothermal software WUFI is used for computations of coupled heat-and-moisture transport (Künzel, 1995). WUFI, which has been validated repeatedly (Kehrer & Schmidt, 2008), features a detailed radiation model, based on physical fundamentals, which calculates the temperatures of the exterior surfaces, thus determining the risk of condensation. In consideration of the

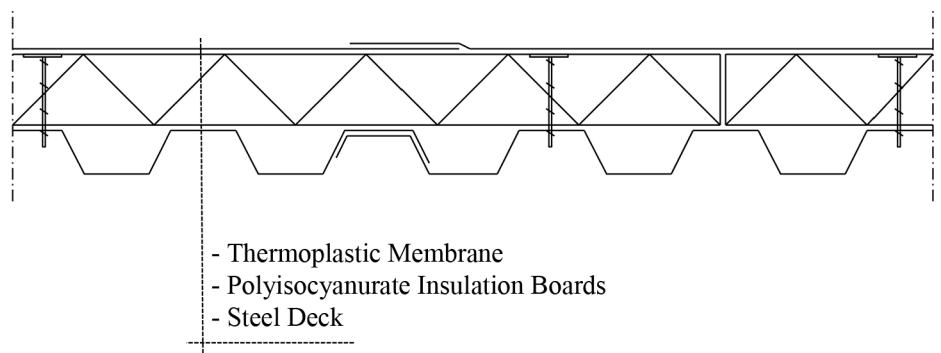


Figure 1 – Model of the investigated mechanically attached roof system. The thermoplastic membrane has either a light or a dark surface that affects the hygrothermal performance of the roof.

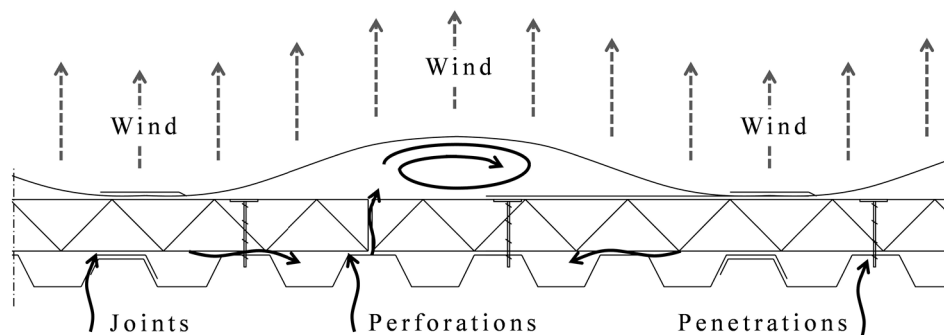


Figure 2 – Wind forces inducing pressure differences on the outer roof membrane, causing the membrane to flutter and balloon. Depending on the condition and workmanship of the structure, air intrusion may arise in overlapping joints of the steel deck, penetrations, or perforations. Plausible locations of air intrusion are indicated with solid arrows. The uplift forces, due to the wind, are indicated with dashed arrows.

expected air intrusion underneath the thermoplastic roof membrane, the air exchange model of WUFI is applied to estimate the heat and moisture exchange of indoor air.

Figure 1 shows the modeled assembly, consisting of a traditional metal deck, 3-in. polyisocyanurate insulation boards, and a thermoplastic membrane (representing a flexible single-ply membrane). Due to supposedly air-leaky roof construction underneath the thermoplastic membrane, an uplift of the exterior membrane will lead to indoor air intrusion. As a consequence of the air intrusion, an air layer is created underneath the membrane.

The risk of condensation in the investigated roof system in Figure 1 depends on several parameters. Their influences on hygrothermal performance are analyzed in a systematic parameter study in which the following input parameters are varied:

- Climate, including wind and solar loads
- Indoor moisture supply
- Air intrusion rate

Varying the parameters leads to 128 different combinations (i.e., scenarios) that are simulated in WUFI. The composition of the combinations and the different variations of input parameters are discussed under “Investigation and Measurements.”

Further, good workmanship is assumed, resulting in a tightly sealed thermoplastic membrane. The mechanical resistance of the membrane is neglected; that is, any applied pressure on top of the membrane is immediately, and without resistance, equalized underneath the membrane.

INVESTIGATION AND MEASUREMENTS

Air intrusion through a roof depends on the wind loads acting on the roof surface and the air permeability of the construction below the thermoplastic membrane. Subsequently, air intrusion is an important parameter to estimate when analyzing the hygrothermal performance of a roof. This section presents an approach to quantify this parameter.

Wind Forces

The airtightness of a roof system, together with the existing pressure differences, determines the air leakage rate between the indoor and outdoor environments. In this study, the thermoplastic membrane is assumed to be sealed with satisfactory workmanship, thus minimizing exfiltration or infiltration air exchange; that is, air will not flow between the inner and outer surfaces of the roof. Instead, the exchange of air inside and between the roof materials is a consequence of indoor air intrusion (i.e., an exchange of indoor air between materials of the building envelope). The air pressure differences influencing the intrusion rate are typically thermally driven (stack effect), with the ventilation system or wind loads acting on the building envelope (Hagentoft, 2001). The wind generally creates an uplift force on the thermoplastic membrane. Due to the flexibility and elasticity of the membrane, it may easily deform in favor of pressure differences, causing the membrane to flutter and balloon (Baskaran & Molleti, 2010). This deformation, due to uplifting forces, is also referred to as billowing (Figure 2).

Two essential parameters must be specified to estimate the air intrusion rate in a roof assembly. One is wind speed fluctuation, which causes a fluctuating pressure difference between the outdoor and indoor surfaces of the roof, and the other is airtightness of the roof structure below the outer membrane.

A negative wind-induced air pressure typically acts on the exterior roof surface and can be estimated by use of ASCE Standard ASCE/SEI 7-10. The wind pressure, P_w , for low-rise buildings is defined in Sections 28.3.2 and 28.4.1. Following the calculation steps of the ASCE standard and determining the suitable coefficients for the roof structure, exposure, and surrounding topography result in an uplift P_w as follows (see Equation 1):

$$P_w = -0.273 \cdot V^2$$

Equation 1

where V (m/s) is the wind speed parallel to the surface.

The wind speed is typically presented as an average speed for a defined period of time (e.g., one hour). Wind speeds that are based on measured averages at shorter time intervals are referred to as gusts, V_g (Harper, Kepert, & Ginger, 2010). Therefore, V can be expressed as Equation 2:

$$V = \frac{1}{m} \cdot \sum_{i=1}^m V_g^i$$

Equation 2

in which m is the number of gust samples within one hour.

In Figure 3, the variations of V and V_g are presented for a period of six hours, extracted from minute-based measurements of the wind speed in Holzkirchen, Germany, from 2009 to 2010.

The difference in wind speed, ΔV , determines the pressure difference. A shorter time step between measured wind speeds is decisive for determining the fluttering effect of the roof membrane, and thus the air intrusion. Unfortunately, climate files usually consist of hourly averages of wind speed in which the differences between high and low wind speeds at shorter time periods are lost, as revealed in Figure 3. Therefore, the hourly averages of data used in this study are adjusted to a normalized minute-based variation of the wind speed. This

procedure estimates a ΔV at a given hourly wind speed, intended to estimate the uplift pressure difference, ΔP_w , acting on the outer membrane surface. The minute-based gust measurements from Holzkirchen, because of their known reliability and continuity, serve as the template for such adjustments. Therefore, the hourly averages of wind speed given from the four U.S. climate zones are adjusted to instead represent a plausible variation of wind speed, ΔV , at each given hour.

The hourly average of ΔV is defined as Equation 3:

$$\Delta V = \frac{1}{m-1} \cdot \sum_{i=1}^m |V_g^{i+1} - V_g^i|$$

Equation 3

In this study, V_g is expressed each minute; hence $m = 60$ and i is the number of consecutive measurements.

Gusts typically decrease with increasing average wind speed (Davis & Newstein, 1968); thus ΔV , which also has been verified with the minute-based gust measurements from Holzkirchen, is taken into account in this study.

Finally, the wind-induced ΔP_w is expressed using [1] and [3]. See Equation 4.

$$\Delta P_w = -0.273 \cdot \left(\frac{1}{m-1} \cdot \sum_{i=1}^m |V_g^{i+1} - V_g^i| \right)^2$$

Equation 4

Air Intrusion

The fluttering effect of the roof sheeting causes an exchange of indoor air underneath the membrane. This air intrusion is defined as an air exchange rate per hour, ACH, and can be defined as Equation 5:

$$ACH = \frac{Q}{V}$$

Equation 5

Figure 3 – Variations of one-minute wind gusts in Holzkirchen, Germany, from 2009 to 2010 and the resulting hourly average wind speeds during the extracted measurements of six hours.

where Q is the airflow rate (m^3/h) and V is the volume of air space that is ventilated (m^3), later assumed to be constant in the numerical model for practical reasons.

Q , in this study, depends on the pressure difference between the membrane and the indoor environment and also on the airtightness of the roof assembly, as given by Equation 6

$$Q = A \cdot C \cdot \Delta P^n$$

Equation 6

where A is the roof surface area (m^2); C is the air leakage coefficient (m^3/s , Pascal [Pa]); ΔP is the pressure difference (Pa), which in this study equals ΔP_w ; and finally, n is the pressure exponent (-). The Q_{50} -value (l/s or l/s/m^2) refers to airflow rate at a pressure difference of 50 Pa, thus simplifying comparisons between different constructions and measurements.

Consequently, C and n are parameters related to the physical structure of the roof that are typically determined by measurements. Therefore, the roof construction defined in this paper's introduction is tested in accordance with the ASTM E2178-11 standard for testing the air leakage rate. The specimen represents the roof construction as defined in Figure 1, except for the exclusion of the outer thermoplastic membrane. The reason for this approach is that the

complete roof assembly is assumed to be very airtight and that the air intrusion rate between the indoor environment and underneath the membrane is to be estimated.

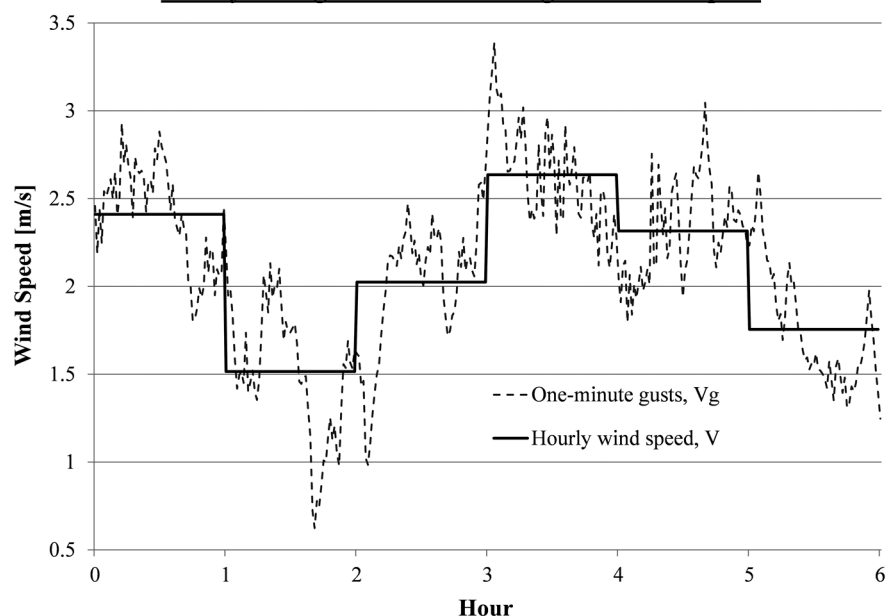
Figure 4 displays the constructed roof specimen. The steel deck includes one overlapping joint and has been screwed tight at three positions along the overlapping ridge, as indicated with solid arrows. Further, two layers of overlapping 1.5-in. insulation boards are mounted on top of the wood-framed steel deck.

The roof specimen was tested in five different assemblies:

1. Sealed joints and sealed screw penetrations
2. Steel deck only
3. Full assembly
4. Full assembly, two to four 3/16-in. steel deck perforations
5. Full assembly, eight 3/16-in. steel deck perforations

The results of the measurements are presented in Table 1, in which the different assemblies were measured with various repetitions. The purpose of the first assembly (sealed joints and sealed penetrations) was to ensure a satisfactory seal between the steel deck and the wooden framework, which is confirmed by the results in Table 1. Second, only the steel deck was tested, without the insulation boards mounted on top. This assembly was later compared with the full assembly with both steel deck and insulation boards, though without the thermoplastic membrane. The results from

Hourly averages and one-minute gusts of wind speed



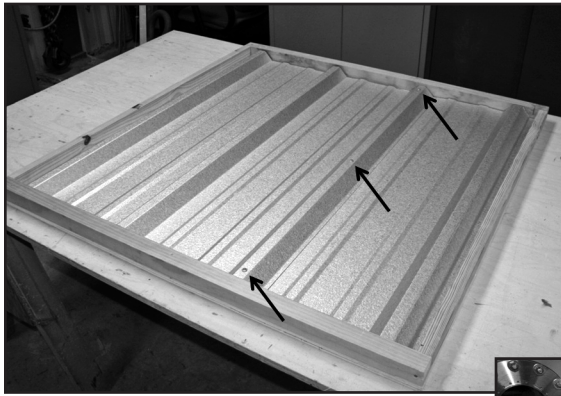
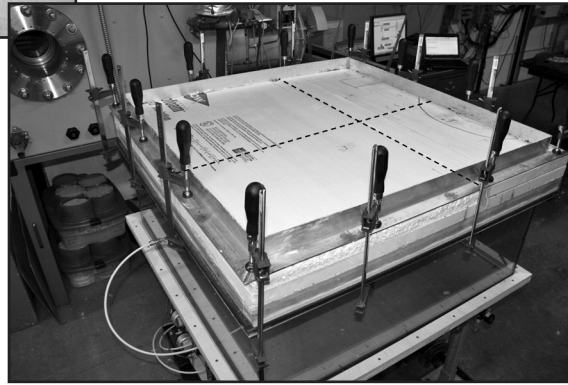


Figure 4 – The airtightness of the materials below the thermoplastic membrane, which was tested by use of ASTM E2178-11. The specimen was constructed with a steel deck including a joint and, on top, two overlapping 1.5-in. insulation boards. The screws, ensuring a tight overlap, are indicated with arrows. The joints between the overlapping insulation boards are indicated with dashed lines in the right-hand picture.



these two assemblies indicate that the airtightness of the steel deck is conclusive (i.e., the airtightness of the insulation boards is much less than that of the steel deck). Further, the steel deck was perforated with various 3/16-in. drilled holes. The effects of a perforated steel deck are presented in *Table 1*, indicating the importance of intact steel sheeting.

The results from measuring the airtightness of the metal roof construction indicate that even small perforations of the steel increase the leakage rate significantly. A well-performed overlap of the steel deck sheets, screwed tight and without further sealing, has relatively high airtightness, however. Noteworthy is that the tested assemblies do not include any installation or structural penetrations that need to be sealed. The IECC-2012 *Standard for Commercial Energy Efficiency* declares the importance of sealing penetrations (ICC,

2011). Further, the IECC standard provides three different approaches to determining the air barrier of different materials, construction assemblies, or the complete building, where the latter shall not exceed 2.0 l/s/m² at a pressure difference of 75 Pa. Assuming an *n*-value of 0.6, this regulation equals a maximum *Q*₅₀-value of 1.57 l/s/m². Naturally, the air leakage regulation includes all parts of the building envelope and not solely the roof. However, steel

decks have been proven leaky, so sealing the joints of the steel sheets and ensuring a nonperforated steel deck is important for overall airtightness (Walsh, 2007). A literature study prepared for the California Energy Commission in 2006 presented an average *Q*₅₀-value of 4.0 l/s/m² based on air leakage tests in 267 commercial buildings (Gadgil, Price, Shehabi, & Chan, 2006).

Another aspect of analyzing the results from the measurements of this study is their expected relationship to constructed roofs. The airtightness of the test specimens and the field measurements have been shown to deviate. Test results of a specimen representing a lightweight compact metal roof without a vapor retarder, like the roof system presented in *Figure 1*, resulted in a *Q*₅₀-value

of about 0.75 l/s/m², though field measurements varied between 2 and 6 l/s/m² (Hens, Zheng, & Janssens, 2003).

In the simulation model, the air layer is assumed to have an average thickness of 3 cm, representing the flutter-induced air cavity.

Further, material properties from the hygrothermal model database are utilized, except for the metal trapezoidal construction, where a vapor permeance of 1.0 (perm)

Results from airtightness tests	<i>C</i> (m ³ /s,Pa)	<i>n</i> (-)	<i>Q</i> ₅₀ (m ³ /s)	<i>Q</i> ₅₀ (l/s)
1. Sealed joints and sealed screw penetrations	3.31E-07	0.99	1.74E-05	0.02
2. Steel deck only	6.45E-06	0.95	2.63E-04	0.26
3. Full assembly	6.19E-06	0.96	2.69E-04	0.27
4. Full assembly, 2–4 perforations	6.85E-05	0.54	5.61E-04	0.56
5. Full assembly, 8 perforations	1.25E-04	0.72	2.09E-03	2.09

Table 1 – Results from measuring the air leakage coefficient, *C*, and the pressure exponent, *n*. Five different assemblies were measured with various repetitions and are presented as average values of the measurements.

is applied. The permeance represents a metal deck including air leakages from penetrations such as screws and is in accordance with earlier investigations done at Oak Ridge National Laboratory (Kyle & Desjarlais, 1994). The initial moisture content of the materials in the simulation model is in accordance with EMC80 (ASHRAE, 2011).

PARAMETERS

The results of this study are based on multiple iterations of the numerical simulation of the roof system with varying input parameters. The varying parameters are presented briefly in the Introduction of this paper and are discussed in detail below.

Climate

Four different U.S. climates are used, representing Climate Zones 4 to 7:

- Climate Zone 4 – Baltimore, MD
- Climate Zone 5 – Chicago, IL
- Climate Zone 6 – Minneapolis, MN
- Climate Zone 7 – Fargo, ND

The chosen climate of each city represents the tenth-percentile coldest climate and is presented with hourly values of temperature, relative humidity, wind speed, solar intensity, etc. These climates are applied to serve as design reference years for the estimation of hygrothermal performance in buildings (Sanders, 1996).

Surface Solar Reflectance

The solar absorptivity of a surface defines the ratio of solar radiation absorbed by a surface and varies between 0 and 1. The solar absorptivity used in the simulations of this study is set to either 0.3 or 0.85, which is representative of a white or a dark surface, respectively. These values assume that a white roof reflects 70% of the sunlight and a dark surface reflects only 15%. The variation in solar absorptivity allows the hygrothermal performance of a cool roof color to be compared to that of a traditional darker roof color. The disparity between the chosen solar absorptivity for the light and dark surfaces in this study is less extreme than in the literature (Bludau *et al.*, 2009), where 0.2 for a white and 0.9 for a black surface are assumed.

Indoor Moisture Supply

Four different variations of indoor relative humidity are used in the simulations.

Variations of Condensate Layer Thickness

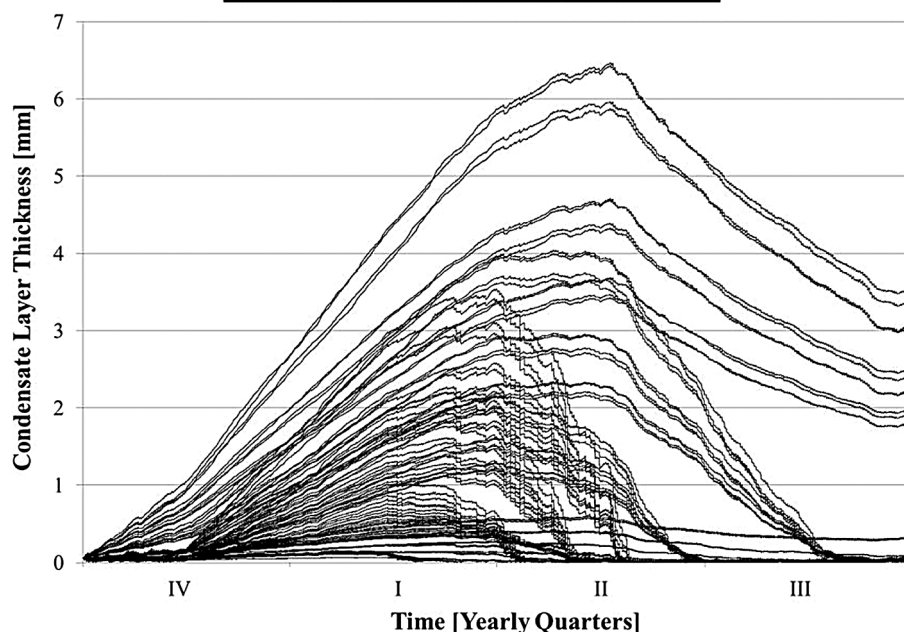


Figure 5 – Condensate layer thickness, d_c , for the 128 simulated roofs with a mechanically attached outer membrane. Typically, the thickness increases during the heating season.

Due to the lack of specific design values for commercial buildings, equivalent rates for residential buildings are applied. The four different variations of indoor moisture supply are presented here:

- EN-15026, where the indoor relative humidity is assumed to vary with the outdoor temperature and is presented in two different classes: normal and high moisture load (Standardization, 2007). The high moisture load of EN-15026 is equivalent to the simplified default indoor design humidity method of ASHRAE 160 (ASHRAE, 2011). This study uses both the normal and the high indoor moisture load.
- ASHRAE 160 intermediate method, where the moisture load depends on the specified number of bedrooms and ventilation ACH. Two different scenarios are chosen for this study: two bedrooms with ACH= 0.6 and six bedrooms with ACH=0.2, which supposedly are representative of low and high indoor moisture, respectively.

Air Intrusion

Typical air intrusion rates are defined under “Investigation and Measurements” (on Page 161). The chosen rates are based on four different leakage rates of the roof assembly, presented below. The air intrusion

rates used in the simulations of the roof are as follows:

- $Q_{50} = 0.27 \text{ (l/s/m}^2\text{)}$ A perfectly assembled roof system with regard to both material properties and workmanship, according to measurements of the air leakage in the roof construction below the thermoplastic membrane in Table 1.
- $Q_{50} = 0.56 \text{ (l/s/m}^2\text{)}$ An assumed satisfactory roof assembly, though with minor perforations in the steel deck; it is based on measuring the average leakage rate with a varying number of 3/16-inch holes (see Table 1).
- $Q_{50} = 1.0 \text{ (l/s/m}^2\text{)}$ Somewhat leak-prone roof construction, arbitrarily chosen.
- $Q_{50} = 2.0 \text{ (l/s/m}^2\text{)}$ Leaky roof, based on both measurements presented in Table 1 and air leakage tests made on commercial buildings with similar roof assemblies (Gadgil *et al.*, 2006; Hens *et al.*, 2003).

The pertinent air leakage coefficient, C , and pressure exponent, n , values are taken from either Table 1 or are calculated by assuming $n=0.65$, which in lieu of provided values usually is a good assumption (Gadgil *et al.*, 2006).

RESULT

A total of 128 different scenarios of the mechanically attached roof system are simulated, with varying input parameters as defined in the “Parameters” section. Each scenario is numerically simulated for a complete year.

The accumulation of moisture in the air layer between the thermoplastic membrane and the insulation board is evaluated since it is closely related to the amount of condensed water in the roof structure. The moisture content of the air layer is converted into a condensate layer thickness, d_i ,

in which the moisture content is assumed to be distributed over the complete surface area. The conversion is made to facilitate hygrothermal analysis of the roof structure and comparisons among the different simulated scenarios. The variations of d_i for each simulation are presented in Figure 5. Typically, d_i increases during the heating season, when the difference between the indoor and outdoor moisture content is the greatest.

The variations of d_i illustrated in Figure 5, give a range of different simulated roofs, without specifying the chosen input parameters of the simulations. The maximum values of d_i for the simulations are given in Figure 6 and Figure 7 as a function of the chosen indoor moisture supply. A curve, with either a black or a white surface, is presented for each moisture supply with varying climate zone and air intrusion rate.

A critical d_i is commonly taken as 0.5 mm to avoid dripping (DIN, 2001; Hens *et al.*, 2003); hence this value is considered an upper maximum for a safe and reliable roof construction. Additionally, a d_i between 0.5 and 1.0 is considered risky, and values beyond are rated as failures in terms of the risk for condensation. The 1.0 threshold is also recommended in a German standard (DIN, 2001); it is stated as an upper limit to avoid gravitational flow, but in the presence of hygroscopic materials only. However, the standard is mainly used for the surfaces of walls with a sloped roof; consequently, water is more easily drained off compared to a flat roof. Hence, the 1.0 threshold can be assumed conservative and thus applicable for this study.

The results of the risk evaluation for the 128 simulations are given in Table 2.

In eight of the 128 roof scenarios, additional simulations were required for a risk evaluation. These eight roof scenarios accumulated moisture, indicating that the annual variation in moisture content will escalate. To confirm this assumption, the eight scenarios were simulated for five years, under the same condition but with an additional climate, instead representing the tenth percentile warmest climate. Four of the eight resimulated roof scenarios reached risky levels, and the other four reached assumed levels of failure. These results are shown in Table 2.

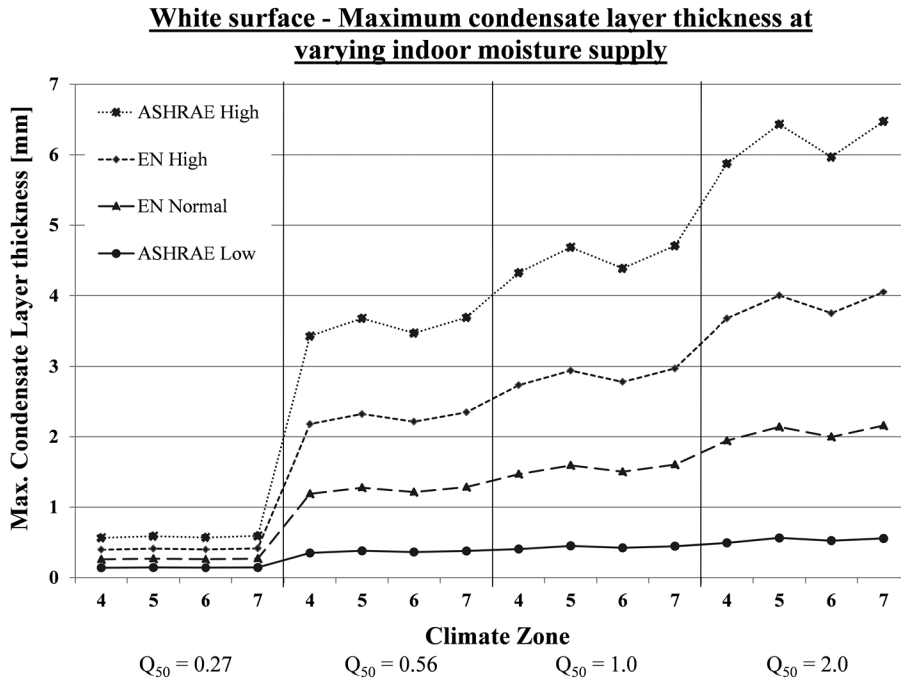


Figure 6 – Maximum condensate layer thickness for each simulated roof construction with a white membrane surface. The curves represent the chosen indoor moisture supply with varying climate and air intrusion rate.

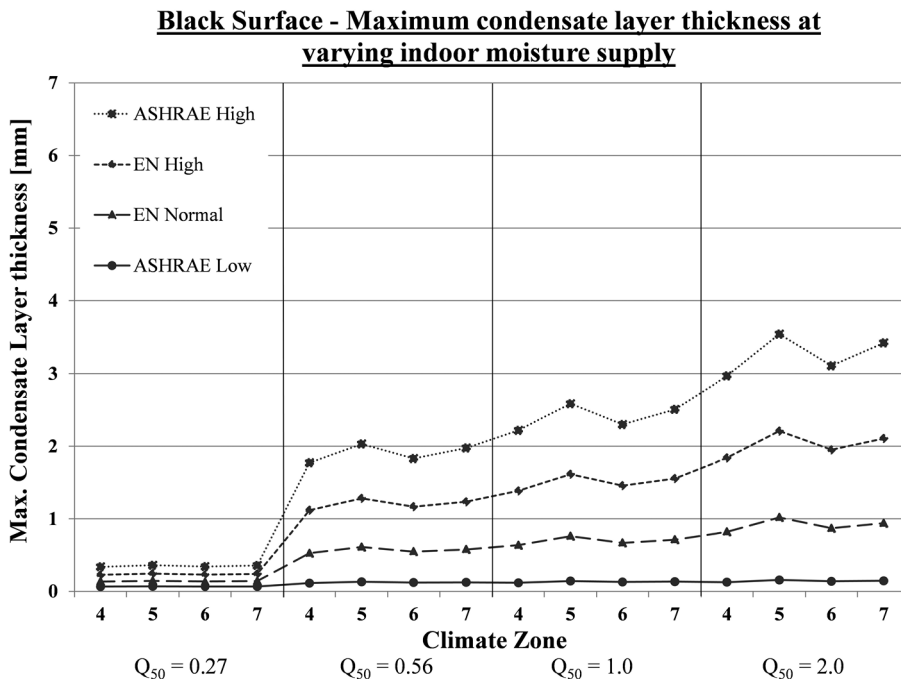


Figure 7 – Maximum condensation layer thickness for each simulated roof construction with a black membrane surface. The curves represent the chosen indoor moisture supply with varying climate and air intrusion rate.

Climate Zone 4								
Indoor moisture supply	Q ₅₀ = 0.27		Q ₅₀ = 0.56		Q ₅₀ = 1.0		Q ₅₀ = 2.0	
ASHRAE - Low	B	W	B	W	B	W	B	W
EN - Normal	B	W	B	W	B	W	B	W
EN - High	B	W	B	W	B	W	B	W
ASHRAE - High	B	W	B	W	B	W	B	W
Climate Zone 5								
Indoor moisture supply	Q ₅₀ = 0.27		Q ₅₀ = 0.56		Q ₅₀ = 1.0		Q ₅₀ = 2.0	
ASHRAE - Low	B	W	B	W	B	W	B	W
EN - Normal	B	W	B	W	B	W	B	W
EN - High	B	W	B	W	B	W	B	W
ASHRAE - High	B	W	B	W	B	W	B	W
Climate Zone 6								
Indoor moisture supply	Q ₅₀ = 0.27		Q ₅₀ = 0.56		Q ₅₀ = 1.0		Q ₅₀ = 2.0	
ASHRAE - Low	B	W	B	W	B	W	B	W
EN - Normal	B	W	B	W	B	W	B	W
EN - High	B	W	B	W	B	W	B	W
ASHRAE - High	B	W	B	W	B	W	B	W
Climate Zone 7								
Indoor moisture supply	Q ₅₀ = 0.27		Q ₅₀ = 0.56		Q ₅₀ = 1.0		Q ₅₀ = 2.0	
ASHRAE - Low	B	W	B	W	B	W	B	W
EN - Normal	B	W	B	W	B	W	B	W
EN - High	B	W	B	W	B	W	B	W
ASHRAE - High	B	W	B	W	B	W	B	W

Table 2 – Results from the 128 simulated scenarios, indicating the reliability of the roof construction at given conditions. Table cells with no background color indicate a safe roof construction, gray indicates risky construction, and black indicates an expected failure with respect to condensation. B stands for a black roof surface, and W stands for white.

DISCUSSION AND CONCLUSION

This study focuses on the risk of condensation in cool roof construction with a mechanically attached outer membrane. The risk evaluation is based on 128 simulated scenarios of plausible roof conditions with varying indoor and outdoor climates. Four input parameters are chosen to vary: the outdoor climate, the solar surface properties, the indoor moisture supply, and the indoor air intrusion rate below the surface membrane.

The results emphasize the importance of solar reflectance at the roof surface. Comparing the maximum condensate layer thickness, d_i , in Figure 6 and Figure 7 reveals that the amount of accumulated moisture is almost doubled in a cool roof construction compared to a traditional black roof.

The indoor moisture supply is very

much related to the expected hygrothermal performance of the roof. Referring to maximum d_i in Figure 6 and Figure 7, a low and a high moisture supply can cause as much as ten times the difference in condensate layer thickness. Another indicator is presented in Table 2, which reveals that only about 10% of the simulated roof is considered risky when the indoor moisture supply is at a low level. (Typically, a low indoor moisture supply is either attained by lowering the moisture production rate or by increasing the ventilation air exchange rate.) A distinction between a white and a black surface with a low moisture supply shows that only a white surface can be risky with a high air intrusion rate. Almost the opposite is valid for high moisture supply, where only about 13% of the roofs are considered safe. Thus,

A low indoor moisture supply or a low air intrusion rate ensures a low risk of intermediate condensation. A safe upper limit of air leakage at 50 Pa, Q_{50} , is stated as 0.17 l/s/m² for metal roofs (Hens *et al.*, 2003). This limit seems consistent with the low risks of the simulated lower air intrusion rate of 0.27 l/s/m², at least for the black roofs of this study. Further, a cool roof will accumulate approximately twice as much moisture below the surface membrane as a black surface. It is assumed that replacing a black surface with a cool membrane on an existing mechanically attached roof system could result in intermediate condensation.

The mechanical resistance of the roof membrane has not been taken into account in this study. Likely, this means that at some lower limit of wind-induced pressure,

only roofs having black surfaces can be considered safe.

The different air intrusion rates show similar behavior in comparison with indoor moisture supply. An increased rate increases the maximum d_i , which also can be seen by the increased slope of the curves in Figures 6 and 7 and by comparing the vertical sections of Table 2.


The fourth variable parameter, the climate, was proven to have the least influence on the amount of accumulated moisture. A slightly increased slope between each climate section in Figures 6 and 7 confirms a small increase in the maximum d_i . The low influence of the specific climate is also obvious by comparing each climate section of Table 2.

In conclusion, both indoor moisture supply and air intrusion rate are critical parameters for hygrothermal cool roof performance.

the uplifting force is lower than the weight and flexible resistance of the membrane, thus preventing any air intrusion. Therefore, a complete depressurization analysis of a mechanically attached roof system is needed to fully analyze a cool roof assembly at realistic and fluctuating wind loads.

It is of major importance to emphasize that a single-ply roof, including an interior vapor retarder, is not necessarily equivalent with an airtight construction. Insufficiently sealed overlaps, perforations, or penetrations of the vapor retarder may cause high air intrusion rates.

Finally, the following practical conclusions can be stated:

- If a very low indoor moisture supply is assumed, no moisture problem is expected, except for white surfaces combined with high air intrusion rates.
- For black roofs, the joints of the steel deck do not necessarily need to be sealed to be considered safe, though penetrations and perforations must.
- The previous statement is only valid for white roofs with low or normal indoor moisture supplies.
- For all other roof assemblies with varying indoor and outdoor climates, an interior air barrier is recommended. 

REFERENCES

- ASCE (2010), Minimum Design Loads for Buildings and Other Structures ASCE/SEI 7-10: American Society of Civil Engineers.
- ASHRAE (2011), ANSI/ASHRAE Standard 160-2009, *Criteria for Moisture-Control Design Analysis in Buildings*. Atlanta, GA: American Society of Heating, Refrigerating and Air-Conditioning Engineers, Inc.
- ASTM (2011a), D7586/D7586M-11, *Standard Test Method for Quantification of Air Intrusion in Low-Sloped Mechanically Attached Membrane Roof Assemblies*: ASTM International.
- ASTM (2011b), E2178-11, *Standard Test Method for Air Permeance of Building Materials*: ASTM International.
- B.A. Baskaran and S. Molleti (2010), "How Much Air Is Too Much?" The National Research Council of Canada Studies of Roof System Air Intrusion: NRC Publications Archive.
- C. Bludau, D. Zirkelbach, and H.M. Kuenzel (2009), "Condensation Problems in Cool Roofs," *Interface*, RCI, Inc., XXVII (7), 11-16.
- F.K. Davis and H. Newstein (1968), "The Variation of Gust Factors With Mean Wind Speed and With Height," *Journal of Applied Meteorology*, Volume 7, Issue 3, pp 372-378.
- DIN (2001), DIN 4108-3, Teil 3: Klimabedingter Feuchteschutz, Anforderungen, Berechnungsverfahren und Hinweise für Planung und Ausführung Wärmeschutz und Energie-Einsparung in Gebäuden. DIN Deutsches Institut für Normung.
- M. Ennis and M. Kehrner (2011), "The Effects of Roof Membrane Color on Moisture Accumulation in Low-Slope Commercial Roof Systems," *Proceedings of NRCA International Roofing Symposium*, 2011, Washington, DC.
- A. Gadgil, P.N. Price, A. Shehabi, and R. Chan (2006), "Indoor-Outdoor Air Leakage of Apartments and Commercial Buildings: Public Interest Energy Research (PIER) Program," California Energy Commission.
- C.E. Hagentoft (2001), *Introduction to Building Physics*, Lund, Sweden: Studentlitteratur.
- B.A. Harper, J.D. Kepert, and J.D. Ginger (2010), *Guidelines for Converting Between Various Wind Averaging Periods in Tropical Cyclone Conditions*: World Meteorological Organization (WMO).
- H. Hens, R. Zheng, and H. Janssens (2003), "Does Performance-Based Design Impact Traditional Solutions? Metal Roofs As an Example," *Proceedings of the 2nd International Conference on Building Physics*, Antwerpen, Belgium.
- ICC (2011), 2012 International Energy Conservation Code: International Code Council, Inc.
- M. Kehrner and T. Schmidt (2008), "Radiation Effects on Exterior Surfaces," *Proceedings of Nordic Symposium on Building Physics*, 2008, Copenhagen, Denmark.
- D.M. Kyle and A.O. Desjarlais (1994), "Assessment of Technologies for Constructing Self-Drying Low-Slope Roofs," Oak Ridge, TN: Martin Marietta Energy Systems, U.S. Department of Energy.
- H.M. Künzel (1995), *Simultaneous Heat and Moisture Transport in Building Components; One- and Two-Dimensional Calculation Using Simple Parameters*, dissertation, University Stuttgart, IRB Verlag. Retrieved from www.wufi.com.
- H.M. Künzel, D. Zirkelbach, and B. Schafaczek (2011), "Vapour Control Design in Wooden Structures Including Moisture Sources Due to Air Exfiltration," paper presented at the 9th Nordic Symposium on Building Physics, NSB 2011, Tampere, Finland.
- S. Molleti, B. Baskaran, P. Kalinger, and P. Beaulieu (2011), "Air Intrusion and Its Effect on Moisture Transport in Mechanically Attached Roof Systems," *Proceedings of the 2011 International Roofing Symposium*.
- C. Sanders (1996), *Annex 24 Heat, Air and Moisture Transfer in Insulated Envelope Parts, Environmental Conditions – Final Report, Volume 2*: ECBCS Annex Publications.
- Standardization, European Committee for Standardization (2007), EN-15026 *Hygrothermal Performance of Building Components and Building Elements – Assessment of Moisture Transfer by Numerical Simulation*: ON Österreichisches Normungsinstitut.
- O. Walsh (2007), *The Essential Guide to Part L of the Building (Amendment) Regulations 2007*, Dublin, Ireland: Navitus Energy Consultants.